Synthesis and Self-Assembly of a Rigid Exotopic Bisphenanthroline Macrocycle: Surface Patterning and a Supramolecular Nanobasket

Venkateshwarlu Kalsani,[a] Horst Ammon,[b] Frank Jäckel,[c] Jürgen P. Rabe,[c] and Michael Schmittel*[a]

Abstract: The synthesis and characterisation of a rigid nanoscale macrocycle with two exotopic phenanthroline binding sites is reported. Scanning tunnelling microscopy (STM) at the solid–liquid interface reveals the formation of highly ordered monolayers of macrocycles with dimensions that are in good agreement with the calculated structure. Using the HETPHEN concept several bisheteroleptic coordination complexes with other phenanthrolines and a nanoscale basket assembly were prepared in presence of copper(I) ions. NMR spectroscopy, mass spectrometric data and elemental analysis point to three distinct isomers of the basket assembly in solution. A silver basket was prepared and readily converted to its copper analogue. Electrospray ionisation (ESI)-MS and spectrophotometric investigations provided additional mechanistic insight into the assembly process. Hence, the exotopic bisphenanthroline macrocycle in combination with HETPHEN concept proves to be very effective in controlling the compositional aspects of multicomponent self-assembly.

Keywords: copper · macrocycles · N ligands · scanning probe microscopy · self-assembly

Introduction

Macrocycles[1] have attracted increasing attention over the last years due to their applicability for surface patterning and as components of supramolecular assemblies. Monolayers of macrocycles on solid supports or interfaces have been suggested to serve as 2D templates for the construction of larger supramolecular 3D assemblies and as matrices for the incorporation of guest molecules.[2–4] These monolayers have been characterised by scanning tunnelling microscopy (STM), Langmuir–Blodgett techniques, X-ray diffraction, photoelectron and infrared spectroscopy as well as ellipsometry.[2–5]

Recently, the synthesis of rigid or shape-persistent macrocycles of nanometer scale has become an important avenue of research.[6] In contrast to ring systems with flexible linkages, a macrocycle with a rigid back bone is an attractive building block for supramolecular architectures to address defined interior and exterior spatial arrangements and relationships. Over the years, rigid macrocycles with or without coordinating ligand sites have been reported.[6] In particular, macrocycles incorporating polypyridyl units have received ample interest due to their coordination properties in presence of suitable metal ions.[7] Schlüter and Grave have reviewed the recent developments on rigid nanosized macrocycles and outlined their assets.[6h] Although many of the rigid macrocycles reported to date contain bipyridine and terpyridine units, most of them (bipyridine) still lack directionality in their coordination behaviour (Figure 1) due to rotational movements, thus allowing for both *exo* and *endo* coordination. For defined *exo* or *endo* coordination phenanthrolines appear superior to bipyridines as a free rotating bond in between chelating nitrogens is fixed. Sauvage, Lüning and others have used flexible macrocycles incorporating endotopic phenanthrolines to engineer functional catenanes, rotaxanes,[8] concave reagents[9] and molecular knots.[10] To the best of our knowledge, the only rigid macrocycle with phenanthroline units has been reported by Rehahn.[11] This macrocycle, however, exhibits endotopic coordination sites, hence prohibiting any access to extended oligomeric structures. Therefore we envisaged the synthesis

[a] V. Kalsani, Prof. Dr. M. Schmittel
Center of Micro and Nanochemistry and Engineering
Organische Chemie I, Universität Siegen
Adolf-Reichwein-Str., 57068 Siegen (Germany)
Fax: (+49) 271-740-4356
E-mail: schmittel@chemie.uni-siegen.de

[b] Dr. H. Ammon
Institut für Organische Chemie der Universität Würzburg
Am Hubland, 97074 Würzburg (Germany)

[c] Dipl-Phys. F. Jäckel, Prof. Dr. J. P. Rabe
Humboldt University Berlin, Department of Physics
Newtonstraße 15, 12489 Berlin (Germany)

Supporting information for this article is available on the WWW under http://www.chemeurj.org/ or from the author.

 DOI: 10.1002/chem.200305770 © 2004 Wiley-VCH Verlag GmbH & Co. KGaA, Weinheim

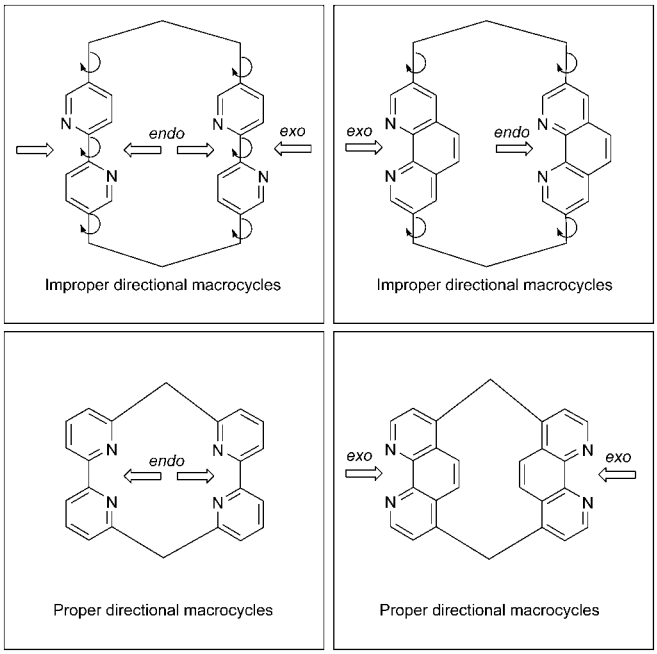

Figure 1. Schematic representation of binding motifs in macrocycles containing bipyridines and phenanthrolines as the coordinating ligands.

of a rigid macrocycle with phenanthrolines that has exotopic coordination sites.

Herein, we present the experimental details of the synthesis[12] of the rigid, nanosized (ca. 2.70 nm length) macrocycle **1** with opposite exotopic phenanthroline sites, its self-assembly studied with scanning tunneling microscopy (STM) at a solid liquid interface and its potential as a useful building block for engineering a heteroleptic supramolecular basket structure through self-assembly in solution along the strategy outlined in Scheme 1.

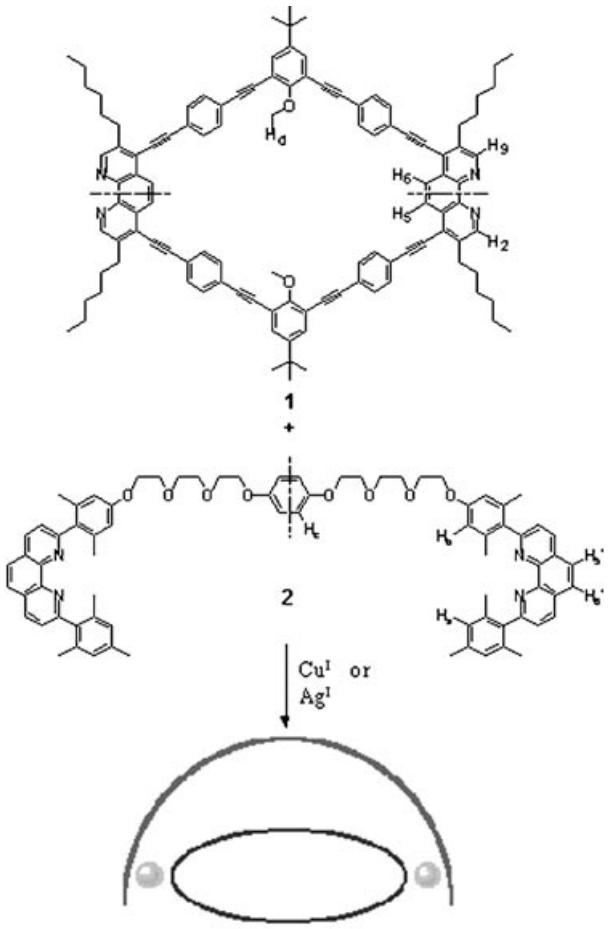

Scheme 1. Schematic representation of the strategy for the self-assembly of a three-component supramolecular basket.

Results and Discussion

Synthesis: Macrocycle **1** was prepared by combining three building blocks by a series of Sonogashira couplings as depicted in Scheme 2 and as communicated earlier.[12] The key building block **3**, equipped with solubilizing hexyl chains in the 3,8-positions,[13] served as source of the exotopic phenanthroline site. Following the synthetic protocol, phenanthroline **3** was first connected with the bisalkyne spacer **4**. After deprotection of **5a**, product **5b** was subsequently linked to two 1,3-diiodobenzene units **6**. Finally, the resultant compound **7** was coupled with **5b** to afford the macrocycle **1**.

Macrocycle **1** precipitated as pale yellow microcrystals in trichloromethane, the structure of which was unambiguously assigned by elemental analysis, ^{1}H NMR spectroscopy, and ESI MS. The ring structure was convincingly visualised by STM.

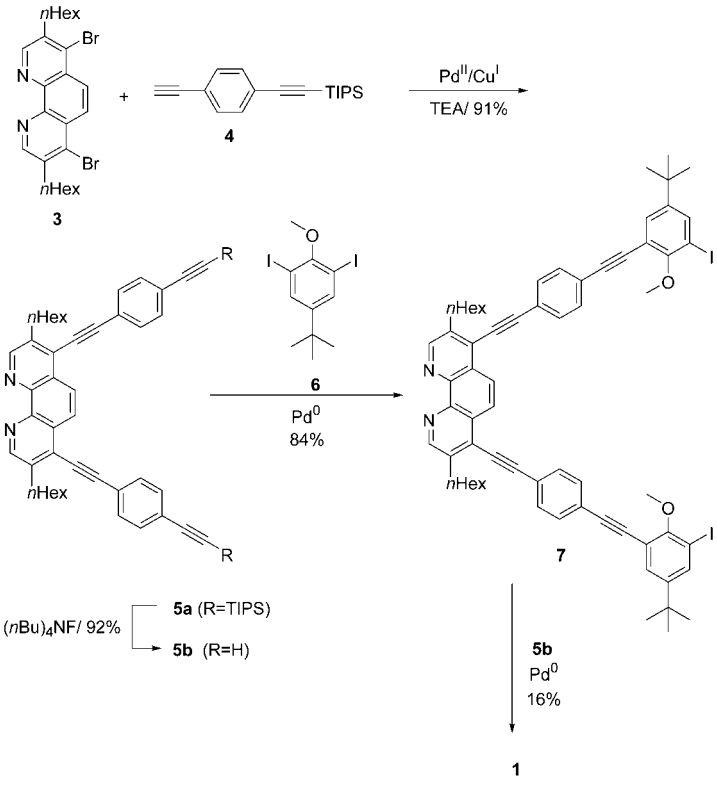

Scheme 2. Preparation of macrocycle **1**.

Synthesis of a handle for a supramolecular basket assembly: The construction of well-defined basket-shaped molecules is of interest, not only because of their potential use in host–guest chemistry, but also to place defined functionalities

© 2004 Wiley-VCH Verlag GmbH & Co. KGaA, Weinheim

above a nanoscale array. While some first cyclophane assemblies have been reported to date,[14] these are well below the nanoscale dimensions. Owing to our earlier results with the HETPHEN concept (allowing for the selective preparation of **het**eroleptic bis**phen**anthroline copper/silver complexes), we chose **2** as a counter part to the macrocycle to prepare the nanoscale basket assembly. The HETPHEN approach[15] utilises steric and electronic effects originating from bulky aryl substituents at one of the two phenanthroline ligands (as seen in **2** and in **10** and **11**) to steer the coordination equilibrium both kinetically and thermodynamically towards the heteroleptic bisphenanthroline complex. Ligands **2**, **10** and **11** are designed to carry steric stoppers at the 2- and 9-positions of the phenanthroline. Ligand **2** was obtained in four steps starting from the parent 1,10-phenanthroline (**8**). The arene groups were added in 2- and 9-position according to Sauvage[16] in a stepwise fashion as depicted in Scheme 3.

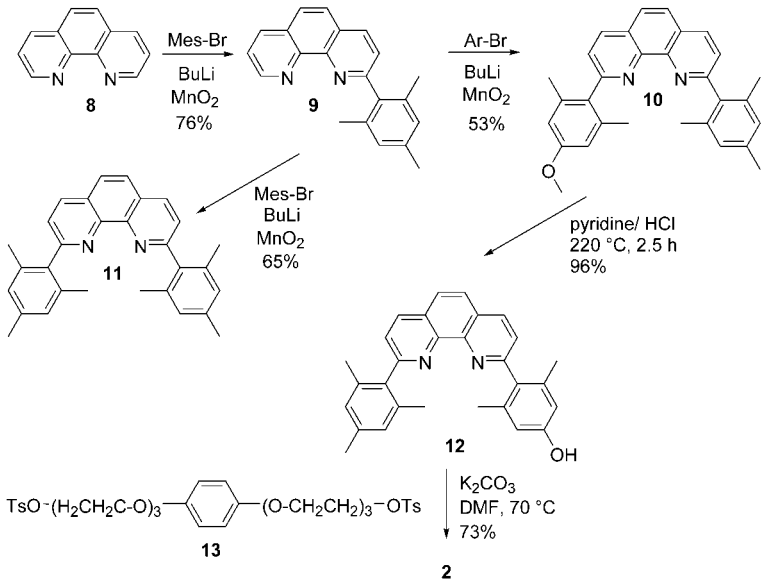

Scheme 3. Synthetic Scheme for the preparation of **2**.

The addition products were isolated and oxidised with activated manganese dioxide to afford the 2,9-disubstituted 1,10-phenanthroline. After deprotection of **10** with pyridine and hydrochloric acid, we obtained the free phenol **12**, which was subsequently treated with **13** to yield **2** in 73%.

Ligand **2** has a ^{1}H NMR spectrum with a singlet at $\delta =$ 6.85 ppm for the four protons of the 1,4-phenylene unit and a ESI MS spectrum with only two signals, one being centred at 1175.7 (25%) $[\mathbf{2}+\mathrm{H}]^+$ and the other at 588.8 (100%) $[\mathbf{2}+2\mathrm{H}]^{2+}$. The isotopic patterns are in agreement with the calculated ones. All other data is also in accordance with its structure (see Experimental Section).

Self-assembly at the solid–liquid interface: Figure 2 displays an STM current image of a highly ordered monolayer of the macrocycle **1** at the solution–HOPG interface (HOPG = highly oriented pyrolytic graphite). The arrangement is characterised by an oblique unit cell containing one molecule ($a = 2.98 \pm 0.15$ nm, $b = 3.08 \pm 0.13$ nm and $\alpha = 47 \pm 6°$). The area of the unit cell of $A = 6.6 \pm 0.3$ nm^2 is in good agreement with the space requirements of a single molecule lying completely flat on the substrate (~6.3 nm^2). The bright areas of the image can be attributed to the conjugated parts of the macrocycle, since the energy difference between the frontier orbital and the Fermi level of the graphite substrate is rather small.[17] The dark areas of the image between the rings can be assigned to the aliphatic side chains that could not be visualised, probably due to their high conformational mobility on a timescale faster than the STM imaging. Notably, also the area inside the rings could be imaged and is probably dynamically occupied by solvent molecules. Owing to the orientation and spacing of the phenanthroline units being ideal for metal ion coordination, one might envisage using these monolayers to study the formation and the electronic properties of coordination polymers.

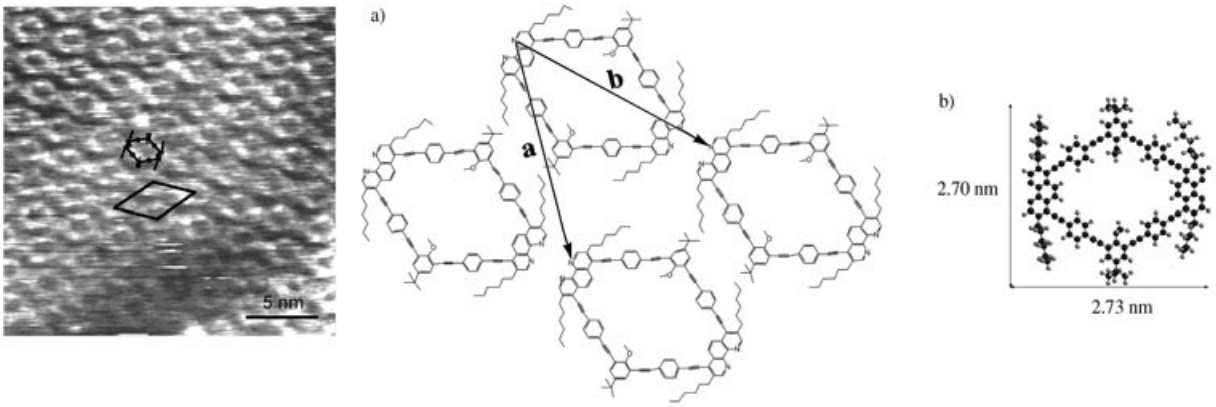

Figure 2. STM current image of a highly ordered monolayer of macrocycle **1**. Parameters were −1.4 V sample bias and 100 pA average tunneling current. Unit cell and macrocycle structure are indicated. a) Model for the arrangement. b) PM3 minimized dimensions of the macrocycle.

 © 2004 Wiley-VCH Verlag GmbH & Co. KGaA, Weinheim

Self-assembly in solution

Complexation behaviour of the macrocycle and of the handle: The presence of two rigid exotopic binding sites renders macrocycle **1** an attractive building block for nanoscale assemblies, particularly in combination with tetrahedrally coordinating metal ions (Cu^+ or Ag^+)[7a] and HETPHEN ligands **2**, **10** and **11**, which contain steric stopper groups in 2,9-position.[15] First, the ability of macrocycle **1** to form complexes with **10** and **11** was probed in presence of Cu^+ (Scheme 4). Rewardingly, only complexes **C1** and **C2**, but no oligomers of macrocycle, could be detected by both ESI-MS and ^{1}H NMR spectroscopy, highlighting the utility of the HETPHEN concept in engineering heteroleptic supramolecular assemblies.

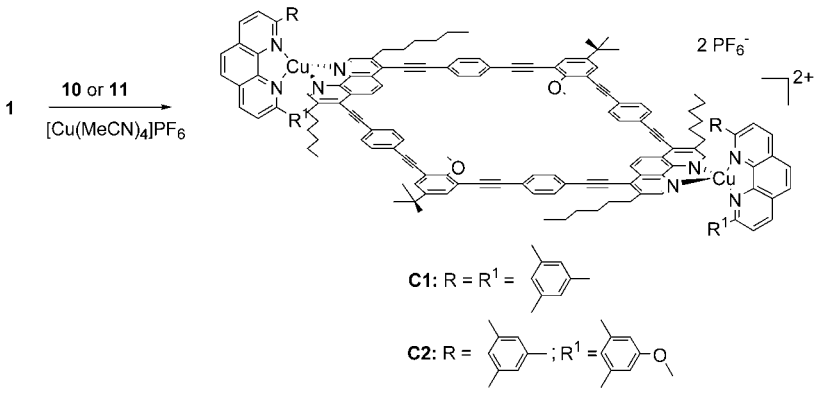

Scheme 4. Formation of complexes **C1** and **C2**.

In the ESI-MS characteristic signals are observed corresponding to **C1** and **C2**, with the experimental isotopic distributions being in good agreement with the calculated ones (Supporting Information: Figure S2). Because of the symmetric structure and the sharp signals, the ^{1}H NMR spectra is readily rationalised. Characteristic high-field shifts were observed for aryl protons of ligands **10** and **11** in the complexes **C1** or **C2**, respectively, a clear indication for formation of heteroleptic complexes as demonstrated earlier.[15]

In the following we probed the complexation behaviour of the handle **2**. A mixture of **2** and $[Cu(MeCN)_4]PF_6$ (1:1) resulted in a yellow solution, the analysis of which by ESI-MS and ^{1}H NMR spectroscopy indicated the presence of mainly $[Cu(\mathbf{2})]^+$ along with unreacted (protonated in case of ESI MS) phenanthroline (Supporting Information: Figure S1a). The isotopic distribution of $[Cu(\mathbf{2})]^+$ is in excellent agreement with the calculated one. However, it is evident from the yellow colour and the absence of any metal-to-ligand charge transfer (MLCT) band in the region of 450–500 nm that no macrocyclic structure with a [Phen-Cu-Phen]$^+$ complex has formed (Supporting Information: Figure S1b).[18] From these experiments it is clear that the two shielded phenanthroline sites act as expected, not allowing for ring closure by formation of a homoleptic ring architecture or any other oligomeric structures.

To create a model complex for comparison with the target basket (Scheme 2), we reacted **2** with **5a** in presence of $[Cu(MeCN)_4]PF_6$ (1:2:2) to furnish **C3** (Scheme 5). ^{1}H NMR spectroscopy, ESI-MS and other spectroscopic data are in good agreement with the proposed structure (see Experimental Section).

ESI MS shows a signal centred at *m/z* 1560.2 Da corresponding to the **C3** complex $[Cu_2(\mathbf{2})(\mathbf{5a})_2]^{2+}$. Again, the experimental isotopic distribution is in good agreement with the calculated one. Formation of complex **C3** is further confirmed by collisional fragmentation of **C3** producing the fragment $[Cu_2(\mathbf{2})(\mathbf{5a})]^{2+}$, whose isotopic distribution is in agreement with its proposed composition (Supporting Information: Figure S3).

Self-assembly of a nanoscale basket assembly and its metal exchange: Following the proposal depicted in Scheme 1, complexation of **1** and **2** with appropriate metal ions such as

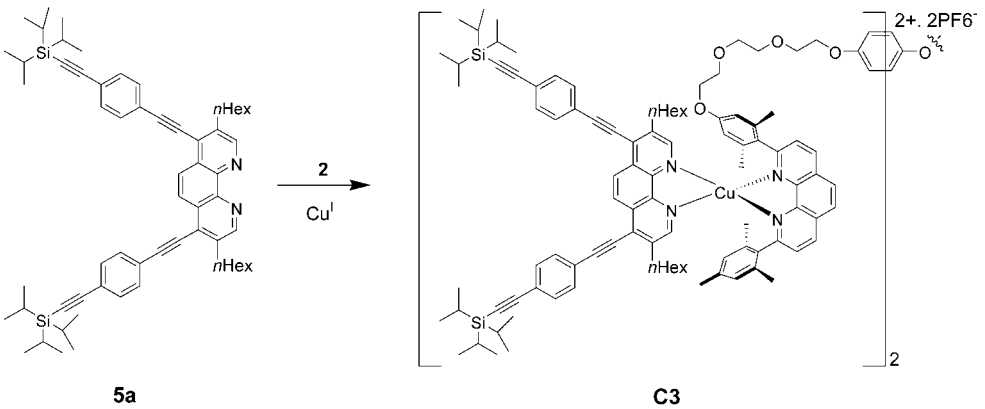

Scheme 5. Assembly of **C3** complex from **2** and **5a**.

© 2004 Wiley-VCH Verlag GmbH & Co. KGaA, Weinheim

Cu^{I} or Ag^{I} ions should furnish a basket-shaped heteroleptic metallo assembly. Upon addition of macrocycle **1** to **2** and $[Cu(MeCN)_4]PF_6$ (1:1:2), the solution turned deep red. The analysis of this solution by ESI-MS indicated the formation of $[Cu_2(\mathbf{1})(\mathbf{2})]^{2+}$ (**C4**) as the exclusive species. The isotopic splitting pointing to a doubly charged species is in perfect agreement with its proposed composition (Figure 3). The ^{1}H NMR spectrum shows that a heteroleptic bisphenanthroline complex has formed at the copper ions, as can be seen from typical high-field shifts of the mesityl and dimethylphenoxy protons at about 5.5–6.3 ppm (Figure 4). The sharp signals in the ^{1}H NMR spectrum rule out the existence of any higher aggregates or oligomers.

*Spectral comparison of **C4** with **C1** and **C2***: The absorption

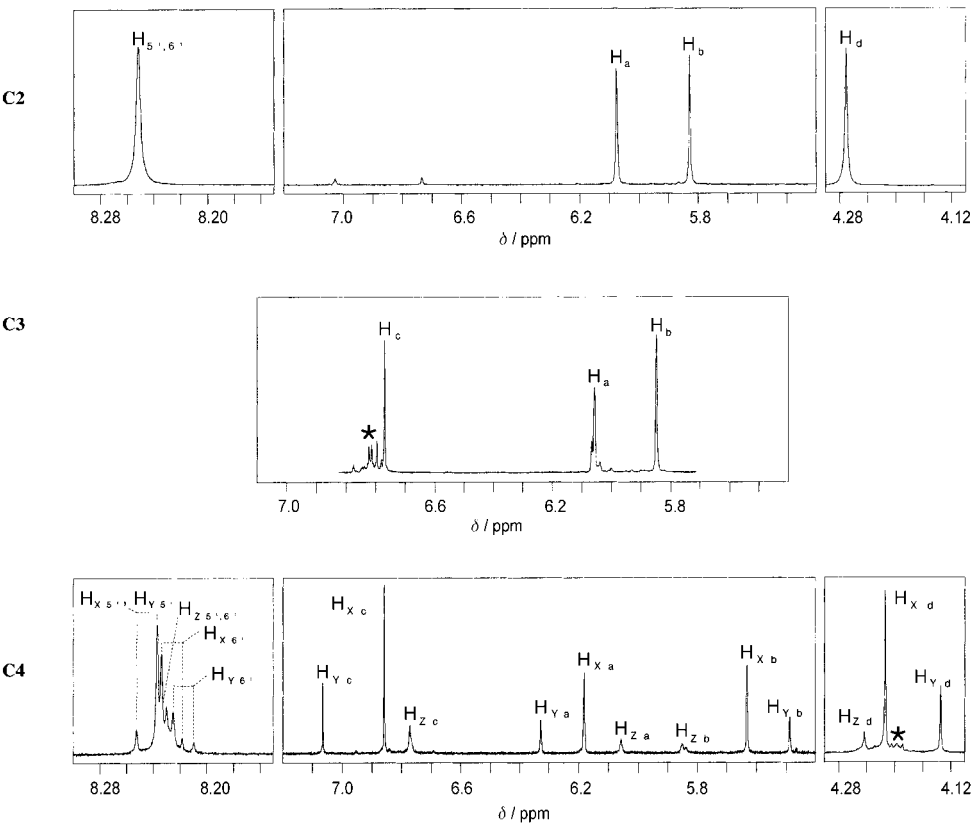

Figure 4. Parts of the NMR spectra (600 MHz) of **C2**, **C3** and **C4**. Complex **C3** shows signals of conformational isomers at H_c and H_a (* = impurity).

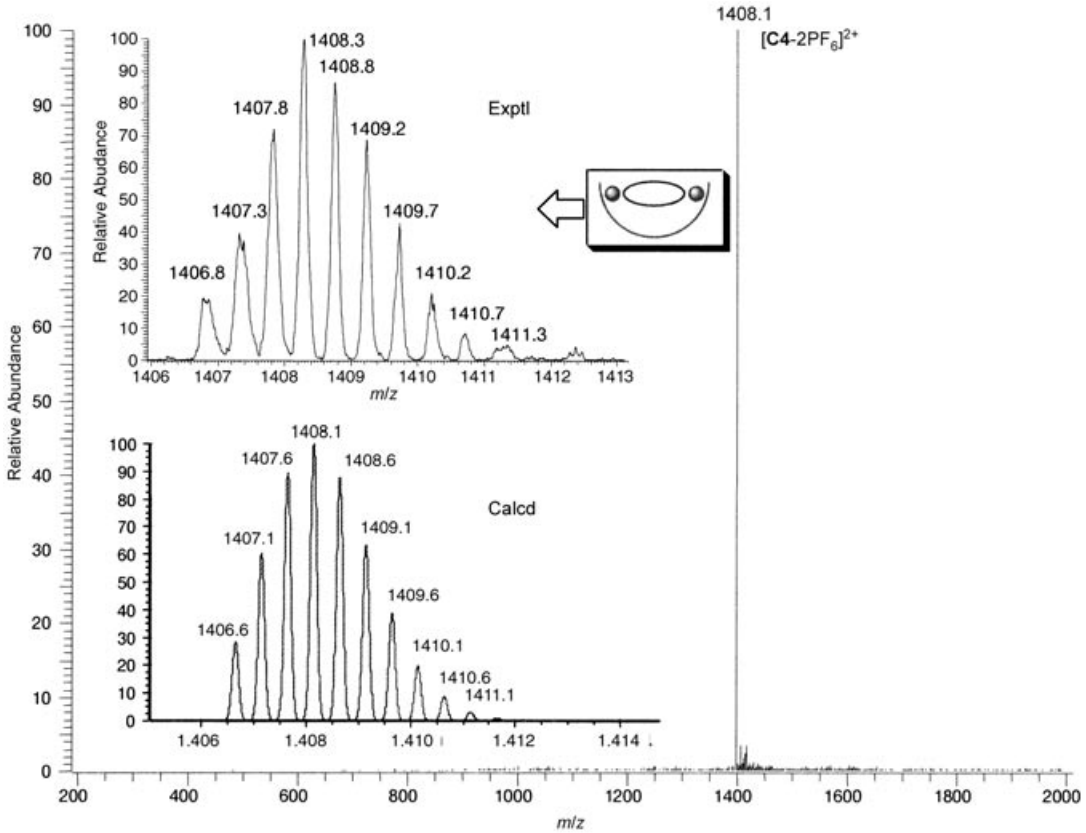

Figure 3. Positive ESI-MS spectrum of $[(\mathbf{1})(\mathbf{2})(Cu)_2]^{2+}$ (**C4**) in dichloromethane. The insert shows the calculated (bottom) and experimental isotopic splittings (top).

 © 2004 Wiley-VCH Verlag GmbH & Co. KGaA, Weinheim

spectra of the heteroleptic complexes **C1**, **C2** and **C4** (Figure 5) show the presence of similar bands. The strong bands at 250–400 nm correspond to ligand π–π transitions.[19]

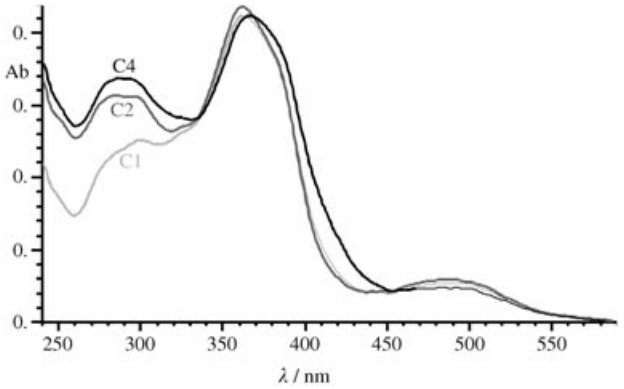

Figure 5. UV-visible absorption spectra of **C1**, **C2** and **C4** (basket assembly) in dichloromethane (2.6×10^{-6} M).

The absorption band at 491 nm is assigned to the MLCT state that is responsible for the red colour of the complexes. These absorptions are in good agreement with those of other Cu^+ heteroleptic bisphenanthroline assemblies.[20] The good match of the MLCT band for all three complexes is indicative of a similar environment at the metal centre. Moreover, the oscillator strength of the MLCT band at $\lambda=$ 491 nm ($\varepsilon_{max}=23113$, 21395 and 18608 $M^{-1}cm^{-1}$ for **C1**, **C2** and **C4**, respectively) is in good agreement with the proposed two Cu^+ ions per complex. Analogous Cu^+-containing systems in which one Cu^+ is present[21] exhibit $\varepsilon_{max}=$ 8500 $M^{-1}cm^{-1}$.

Although ESI-MS and UV-visible data provide a clear and convincing picture for the composition of **C4** as $[(\mathbf{1})(\mathbf{2})(Cu)_2]^{2+}$, the ^{1}H NMR spectra of the complex between 5.5–7 ppm is much more complex than expected, revealing three well-resolved sets of signals (in 59:24:17 ratio;[22] Figure 4). In particular, protons H_a, H_b, H_c and H_d (see Scheme 1) appear well separated, indicating only very slow interconversion between the different isomers. The isomers will be depicted as **C4x**, **C4y** and **C4z**.

Structural aspects: Further information about the structure of the isomers can be deduced from extensive ROESY investigations (Supporting Information: Figures S6 and S7). For one set of the signals (indicated by z; assigned to **C4z**) there is no NOE effect between H_{zc} and H_{zd}, indicating that the ether bridge is well away from the macrocycle (>6 Å), in agreement with a basket type structure (Figure 6, and model **I** in Scheme 6) of **C4z**. In addition, all signals of **C4z** show a remarkable similarity in the shifts with those of the complexes **C2** and **C3** (Figure 4), for which we have to assume an unconstrained polyether chain and a planar macrocycle, respectively. Hence, **C4z** is best described by the basket structure as depicted by an energy-minimised structure from force field calculations (Figure 6 top).[23]

However, **C4z** is only the minor constituent of three different complexes with the same composition $[(\mathbf{1})(\mathbf{2})(Cu)_2]^{2+}$.

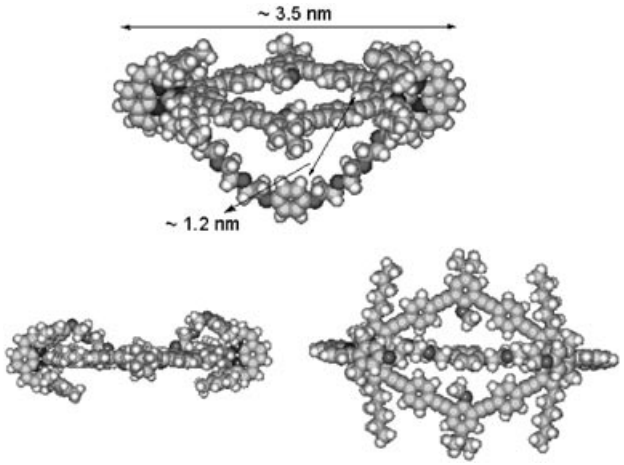

Figure 6. Energy-minimised structure of the basket assembly **C4z** (top), indicating that H_{zc} of **2** and H_{zd} of **1** are far away from each other in line with NOESY data. The structure of **C4xy** is expected to look like the isomer shown in the two bottom pictures (left = side view; right = top view). Conformational motions of the entangled polyether chain in **C4xy** to generate **C4z** are prevented by a high barrier due to the restricted space in the core of the macrocycle.

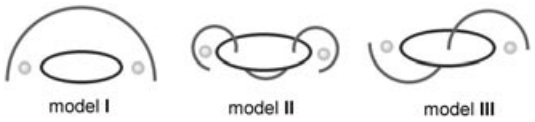

Scheme 6. Cartoon representation of possible isomers of $[Cu_2(\mathbf{1})(\mathbf{2})]^{2+}$ (**C4**).

By chromatography we could separate **C4z** from **C4x**,**y** (^{1}H NMR spectra of isolated **C4x**,**y** and **C4z** are included in the Supporting Information: Figure S8) and confirm the composition $[(\mathbf{1})(\mathbf{2})(Cu)_2]^{2+}$ for both fractions by ESI-MS.

How can we rationalise the occurrence of various isomers of the composition $[(\mathbf{1})(\mathbf{2})(Cu)_2]^{2+}$? Depending on the spatial arrangement of the polyether chain in **C4** there may exist different isomers as depicted in Scheme 6. From these choices the rotaxane-type model **III** can easily be discarded, owing to a rather high barrier (as predicted by molecular modelling[23]) needed for threading the bulky diarylphenanthroline unit of **2** into macrocycle **1** (Supporting Information: Figure S5). The high barrier is mainly due to repulsion of the 2,6-dimethylphenyl groups at phenanthroline of **2** and the methoxy groups in **1**.

In contrast to signal set z, the other two sets of signals, that is, for **C4x**,**y**, show notable NOE effects between H_c and H_d protons; this indicates close proximity of the polyether bridge and the macrocycle, as depicted in a cartoon-type fashion in model **II**. In support of a model **II** type structure for both **C4x** and **C4y**, protons H_{xa} and H_{ya} have signals that are shifted down-field with respect to H_{za}, while the signals for protons H_{xb} and H_{yb} are shifted to high-field with respect to H_{zb}. This can only be rationalised by a distorted geometry at the copper(I) ion, with the dimethylphenoxy unit being closer to the phenanthroline of **1** than the mesityl unit. This is due to a severe conformational pull exerted by

© 2004 Wiley-VCH Verlag GmbH & Co. KGaA, Weinheim

the polyether chain that is entrapped in the macrocycle as shown in model **II**. It is, however, impossible to provide exact conformational differences along the polyether chain of **2** distinguishing the two isomers **C4x** and **C4y**, in particular, since also a slight folding of the macrocycle may be involved.[24] The interconversion between **C4x** and **C4y** occurring at temperatures higher than −20 °C precluded chromatographic separation.

A key for further understanding is to picture the formation of the basket assembly. Upon formation of the mononuclear complex $[(\mathbf{1})(\mathbf{2})(\mathrm{Cu})]^+$ (Scheme 7) the free 2,9-diarylsubstituted phenanthroline site of **2** has actually only two major trajectories[25] to move towards the second phenanthroline of macrocycle **1**: either it stretches the polyether chain to such an extent that approach of the loose phenanthroline along trajectory **A** is possible. Alternatively, the polyether chain may fold partly into the macrocycle due to stabilizing interactions[26] between the handle and the unsaturated macrocycle. This will severely limit the translational freedom of the loose binding site of **2** leaving only trajectory **B** to form the second copper complex.

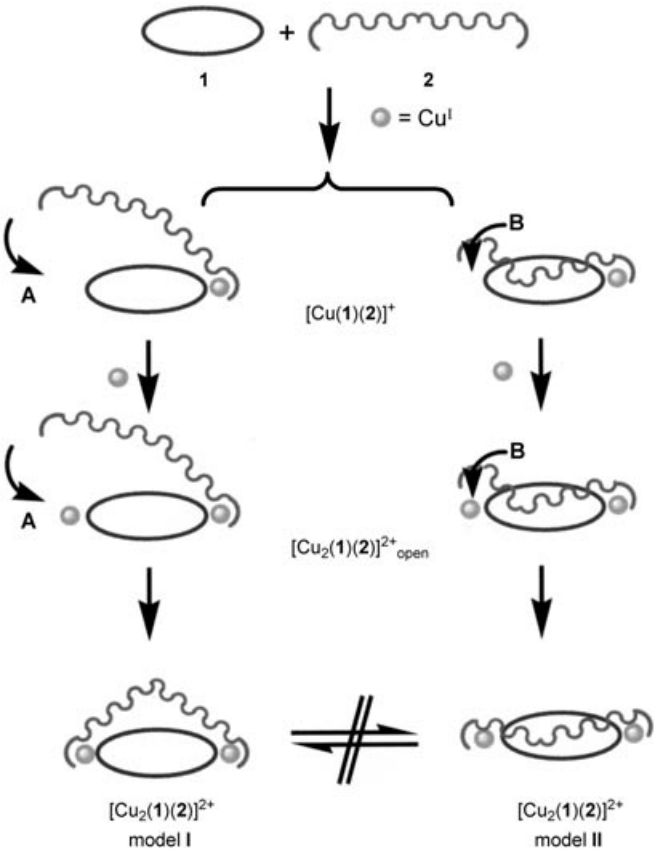

Scheme 7. Cartoon representation of the formation of $[Cu_2(\mathbf{1})(\mathbf{2})]^{2+}$ (**C4**) leading to two sets of isomers (models **I** and **II**).

It is, however, surprising to learn that even at temperatures as high as 60 °C interconversion between **C4x**,**y** and **C4z**, that is, between model **I** and **II** isomers, remains completely shut down. Such a high barrier can only be rationalised if interconversion of **C4x**,**y** and **C4z** is not possible by conformational changes along the polyether chain. Molecular modelling indeed proposed that the entanglement of the cramped polyether chain within the void of the macrocycle will preclude conformational relaxation (Figure 6). Alternatively, a dissociation/association process connecting $[Cu_2(\mathbf{1})(\mathbf{2})]^{2+} \rightleftharpoons [Cu_2(\mathbf{1})(\mathbf{2})]^{2+}{}_{open}$ could potentially bring about the conformational flexibility needed for interconversion (cf. to Scheme 7), but apparently the exergonic association $[Cu_2(\mathbf{1})(\mathbf{2})]^{2+}{}_{open} \rightarrow [Cu_2(\mathbf{1})(\mathbf{2})]^{2+}$ kinetically outruns the slow escape of the conformationally locked polyether chain. If the above rationale was correct, addition of ligand **14**[27] to **C4** should lead to a competitive binding of **14** to $[Cu_2(\mathbf{1})(\mathbf{2})]^{2+}{}_{open}$, thereby freeing the hitherto kinetically locked equilibration between **C4x**,**y** and **C4z**. Indeed, after adding one mole equivalent of **14** to **C4x**,**y**,**z** we saw enrichment of **C4x**,**y** at the expense of **C4z**, while parallel the new complex $[Cu_2(\mathbf{1})(\mathbf{14})_2]^{2+}$ was formed (Scheme 8). This result suggests that dissociation/association at the copper phenanthroline site in pure **C4x**,**y**,**z** takes place, but does not lead to interconversion of the isomers due to entrapment of the polyether chain in the void of the macrocycle. Moreover, this experiments indicates that model **II** structures are thermodynamically more stable than the basket (model **I**) owing to attractive interactions.[26]

Metal exchange: A silver basket was made by mixing **1** and **2** with $AgBF_4$ in dichloromethane, affording a yellowish solution. Analysis of this by ESI MS indicated a signal at $m/z = 1452.2$ with a charge 2+. Isotopic splitting was in good agreement with its proposed composition $[Ag_2(\mathbf{1})(\mathbf{2})]^{2+}$. The ^{1}H NMR spectrum of $[Ag_2(\mathbf{1})(\mathbf{2})]^{2+}$ again indicated the presence of three isomers in a similar ratio as for the $[Cu_2(\mathbf{1})(\mathbf{2})]^{2+}$ complex. Upon the addition of $[Cu(MeCN)_4]^+$ in dichloromethane (2 equiv, 8 additions, 30 min), the $[Ag_2(\mathbf{1})(\mathbf{2})]^{2+}$ was quantitatively converted to $[Cu_2(\mathbf{1})(\mathbf{2})]^{2+}$. In the conversion process, signals of the intermediate species $[AgCu(\mathbf{2})(\mathbf{1})]^{+2}$ were detected (Supporting Information: Figure S4). Importantly, the conversion of $[Ag_2(\mathbf{1})(\mathbf{2})]^{2+}$ to $[Cu_2(\mathbf{1})(\mathbf{2})]^{2+}$ does not entail detectable changes in the com-

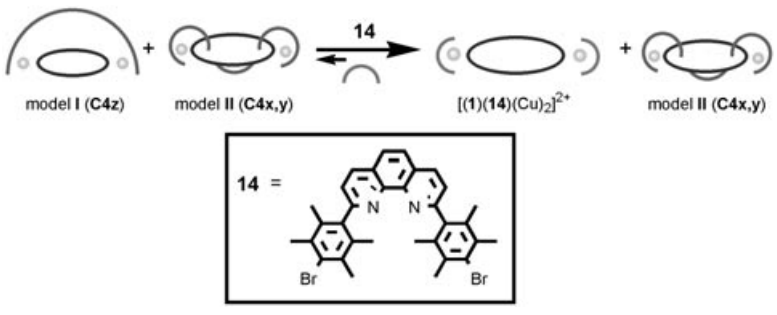

Scheme 8. Competitive binding of ligand **14**.

 © 2004 Wiley-VCH Verlag GmbH & Co. KGaA, Weinheim

position **C4x**:**C4y**:**C4z**. Hence, metal exchange after dissociation followed by association is faster than conformational relaxation from model **I** to model **II**.

ESI MS investigations, thermodynamic and UV-visible studies: Insight into the mechanistic pathways and thermodynamic features of supramolecular structures is of great interest to engineer well-defined, discrete architectures and to understand the self-recognition phenomena. Very few reports are at hand providing mechanistic insight into the heteroleptic organisation.[14a,28] The present study uses ESI MS for qualitative analysis and spectrophotometry for quantitative analysis. Both measurements were carried out in dichloromethane, which we have found is a good solvent for such titrations.[29] At first, a series of ESI MS titration experiments was carried out to obtain a qualitative picture about the intermediates on the way to $[Cu_2(\mathbf{1})(\mathbf{2})]^{2+}$. In each case, it was ascertained that the thermodynamic equilibrium had been reached, as the spectra recorded proved to be constant over time. A table of the results is presented in the supplementary material.

*ESI-MS titration of **2** and Cu^+ with **1***: In a first series of experiments **2** and the Cu^I salt were titrated with **1**. The titration was carried out in five additions and excess addition of **1** did not effect $[Cu_2(\mathbf{1})(\mathbf{2})]^{2+}$, indicating a high stability of this assembly under the chosen conditions. During the course of titration four intermediates were observed apart from the final basket-shape assembly. All the proposed intermediates (see the pictorial description in Scheme 9) were in good agreement with their isotopic splittings and served as models for the spectrophotometric titration using SPECFIT[30] program.

Scheme 9. Proposed species (cartoons) in equilibrium when **2** and Cu^+ were titrated with **1**.

*ESI-MS titration of **2** and **1** with Cu^+*: The second series of experiments was carried out by the titration of **2** and **1** with the Cu^I salt. The Cu^I salt (two equivalents) was added in five portions. Again, excess of addition did not change the spectrum. Though it was possible to detect three intermediates in minute amounts, the final basket assembly appeared as the major component throughout the titration, indicating a strong tendency to form $[Cu_2(\mathbf{1})(\mathbf{2})]^{2+}$. The obtained results are presented in Scheme 10.

*ESI-MS titration of **1** and Cu^+ with **2***: Finally in a third set of titrations, **1** and the Cu^I salt were titrated with a solution of **2**; the obtained results are depicted in Scheme 10 along with their proposed structures. Due to the starting conditions with macrocycle **1** being present along with Cu^+, homoleptic assemblies were observed in absence of **2**. These, however, readily disappeared upon addition of **2**, indicating the higher stability of the heteroleptic basket assembly Scheme 11

Scheme 10. Proposed species (cartoons) in equilibrium when **1** and **2** were titrated with Cu^+.

Scheme 11. Proposed species (cartoons) in equilibrium when **1** and Cu^+ were titrated with **2**.

*UV-visible titration of **2** and **1** with Cu^+*: The ESI-MS titrations suggest a qualitative picture of the intermediates in the self-assembly process. Though, the mechanistic pathways vary with the type of titration, they always lead to $[Cu_2(\mathbf{1})(\mathbf{2})]^{2+}$ as the final complex. Because of the simplicity observed with the second series of titration experiments with ESI-MS, the same type of titration was carried out for spectrophotometric studies. Hence, these titrations were performed by titrating **2** ($3.3\ 10^{-6}$ M) and **1** ($3.3\ 10^{-6}$ M), with aliquot amounts of a solution of Cu^I in dichloromethane for 20 additions (total 4 equiv of Cu^+). Figure 7 displays changes in UV-visible spectrum upon Cu^I salt addition, with the solution turning red due to the MLCT transitions at ~490 nm. The inset shows the plots of absorbance changes at 490 nm for **2** and **1** versus Cu^I salt, indicating that the complexation process is finished when two equivalents of Cu^I salt are added and excess addition of Cu^+ does not effect

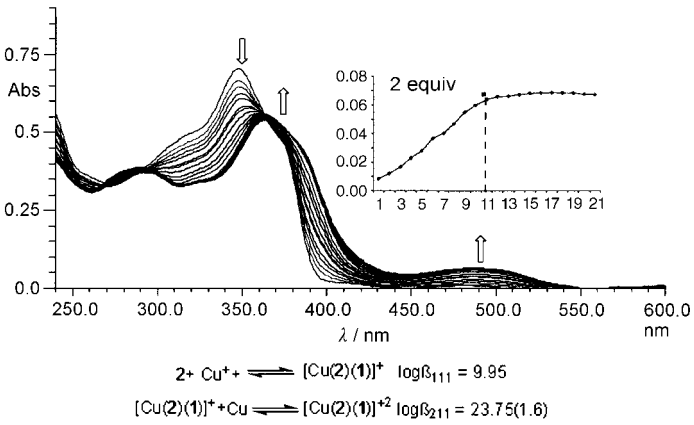

Figure 7. Spectrophotometric titration of **2** and **1** by aliquot amounts of Cu^I salt in 20 additions. Solvent: dichloromethane. $T = 25(1)°$; [**2**] and $[\mathbf{1}] = 3.30 \times 10^{-6}$ M. Stability constants are given down to UV-visible spectra.

© 2004 Wiley-VCH Verlag GmbH & Co. KGaA, Weinheim

the already formed basket assembly. Fitting the model with UV-visible data using the SPECFIT program,[30] binding constants could readily be extracted for complexes $[Cu(\mathbf{2})(\mathbf{1})]^+$ and $[Cu_2(\mathbf{2})(\mathbf{1})]^{2+}$. As depicted in Scheme 10 a two step pathway is postulated for the basket assembly process. Although the $\log\beta_{111}$ value is in the range of similar Cu^+ species,[25] the $\log\beta_{211}$ value is relatively high, indicating the cooperativity in the final step.

Conclusions

We report the synthesis of the rigid nanoscale macrocycle **1**, its self-assembly behaviour at a solid–liquid interfaces and its usage in building a heteroleptic supramolecular nanoscale basket through self-assembly in solution. The presence of two rigid exotopic bidentate chelating groups makes **1** a useful building block to create nanoscale architectures. On one side, STM shows highly ordered monolayers of the macrocyclic system **1** at the solution–HOPG interface. On the other side, there is a strong driving force for this macrocycle to form selectively heteroleptic Cu^+ and Ag^+ complexes with other phenanthrolines. The formation of these complexes is confirmed by a multitude of spectroscopic techniques (see Experimental Section). Most interesting is the formation of a heteroleptic self-assembled basket-shaped aggregate that shows up in three different isomeric structures. The mechanistic investigations led to the proposal of a two step pathway for the self-assembly process. In addition, the conversion of the silver to the copper basket demonstrates the system to be dynamic. Further studies are in progress to study the interface behaviour of self-assembled structures of **1** with metal ions, host–guest properties of these assemblies and the construction of higher order supramolecular aggregates.

Experimental Section

Starting materials 1,10-phenanthroline, ethynyltrimethylsilane, ethynyltriisopropylsilane, 2-bromo-1,3,5-trimethylbenzene, 2-bromo-5-methoxy-1,3-dimethylbenzene, 4-bromophenylamine, activated MnO_2 and 4-*tert*-butylphenol were purchased from Aldrich, Merck or Lancaster and used as received. $[Pd(Ph_3P)_2Cl_2]$,[31] $[Pd(Ph_3P)_4]$,[32] **3**,[13] **9**,[15a] **11**,[15b] (4-bromophenylethynyl)trimethylsilane[34] and 5-*tert*-butyl-1,3-diiodo-2-methoxybenzene[35] were prepared according to the literature procedures. Standard inert atmosphere and Schlenk techniques were employed for all the Heck reactions. Solvents were dried using typical drying procedures. ^{1}H NMR and ^{13}C NMR spectra were measured on a Bruker AC200 (200 MHz) or Bruker AMX600 (600 MHz). All the ^{1}H NMR spectra were carried out at room temperature in deuterotrichloromethane unless specified otherwise. ESI MS was measured on an LCQ Deca Thermo Quest instrument. Typically, each time 25 scans were accumulated for one spectrum. UV-visible spectra were recorded on a Tidas II spectrophotometer with dichloromethane as the solvent. For full characterisation of **4** and its immediate precursor see reference [33]

STM at the solid–liquid interface[34] was performed by using a home-built beetle-type STM interfaced with a commercial controller (Omicron). STM tips were prepared by mechanically cutting a 0.25-mm thick Pt/Ir (80%/20%) wire. A drop of an almost saturated solution of the macrocycle in 1,2,4-trichlorobenzene was applied to the basal plane of freshly cleaved highly oriented pyrolytic graphite (HOPG). The lattice of the underlying substrate could be visualised during measurements by simply changing the tunneling parameters to small tunneling impedance. This allows in-situ *x*,*y* calibration of the piezo-scanner and drift-correction of the images recorded.

Molecular modelling was done with the MM+ force field as implemented in Hyperchem 6.02.[23]

Spectrophotometric titrations: Equilibrium constants of complexes were determined in dichloromethane. Macrocycle **1** and **2** were titrated with aliquot amounts of a stock solution of copper(I) tetrakisacetonitrile hexafluorophosphate. All stock solutions were prepared by careful weighing on a μg analytical balance. Absorption spectra were recorded at 25.0 ± (0.1) °C. Since the formation is instantaneous as evidenced by proton NMR spectroscopy, ESI-MS analysis, and visible colour change, the solutions were immediately analysed by the spectroscopy to avoid problems with the volatile solvent. The wavelength region from 240 nm to 600 nm was taken into account. Two equivalents (total) of metal salt in dichloromethane solution were added in 20 portions. The entire data sets comprising absorbances measured in one nanometer steps were decomposed in their principal components by factor analysis, and subsequently the formation constants including their standard deviation were calculated by using the SPECFIT[30] program. Binding constants were determined from two independent titrations.

Synthesis of 7

3,8-Dihexyl-4,7-bis-{4-[(trisisopropylsilyl)ethynyl]phenylethynyl}-1,10-phenanthroline (5a): Compounds **3**[13] (1.00 g, 1.98 mmol) and **4** (1.73 g, 6.12 mmol), $[PdCl_2(PPh_3)_2]$ (150 mg, 210 μmol) and CuI (300 mg, 1.60 mmol) were placed in a dry flask and dry benzene (20 mL) and dry triethylamine (10 mL) were added in an inert atmosphere. The resulting dark solution was refluxed for 3 d and the solvent was removed under reduced pressure. The residual material was dissolved in dichloromethane (50 mL) and washed with aqueous KCN (50 mL, 20%) and later by water. The solvent was then removed under reduced pressure. The residue was purified by column chromatography with dichloromethane and subsequently ethyl acetate as eluents to afford 1.64 g (90%) of **5a** as yellow powder. M.p. 67–70 °C; ^{1}H NMR (200 MHz): $\delta = 0.87$ (t, $J =$ 6.9 Hz, 6H; hexyl), 1.05 (s, 6H; triisopropyl), 1.15 (s, 36H; triisopropyl), 1.23–1.54 (m, 12H; hexyl), 1.72–1.90 (m, 4H; hexyl), 3.07 (t, $J = 6.6$ Hz, 4H; hexyl), 7.53 (d, $J = 8.6$ Hz, 4H; phenyl), 7.60 (d, $J = 8.6$ Hz, 4H; phenyl), 8.38 (s, 2H; phenanthroline), 9.04 ppm (s, 2H; phenanthroline); ^{13}C NMR (50 MHz): $\delta = 11.3$, 14.0, 18.7, 22.6, 29.2, 30.6, 31.6, 32.6, 85.7, 93.8, 101.9, 106.4, 122.2, 124.5, 125.1, 127.6, 127.7, 131.5, 132.2, 138.9, 144.4, 151.2 ppm; IR (KBr): = 2941, 2863, 2204, 2153, 1560, 1508, 1459, 1420, 1382, 1232, 996, 882, 835, 677 cm^{-1}; elemental analysis calcd (%) for $C_{62}H_{80}N_2Si_2{\cdot}H_2O$ (927.52): C 80.29, H 8.91, N 3.02; found: C 80.21, H 8.62, N 3.14.

4,7-Bis-(4-ethynylphenylethynyl)-3,8-dihexyl-1,10-phenanthroline (5b): Tetrabutylammoniumfluoride trihydrate (1.04 g, 3.30 mmol) in THF (50 mL) was added to a solution of **5a** (1.25 g, 1.35 mmol) in THF (50 mL). The resulting mixture was stirred at room temperature for 30 min; then the reaction was quenched by the addition of water (100 mL). The resulting solution was extracted with dichloromethane and the combined organic layers were dried over $MgSO_4$. The solvent was removed under reduced pressure and the residue was purified by column chromatography with dichloromethane and then ethyl acetate as eluents to give 750 mg of **5b** (92%) as ochre coloured crystals. M.p. 173–174 °C; ^{1}H NMR (200 MHz): $\delta = 0.87$ (t, $J = 6.9$ Hz, 6H; hexyl), 1.21–1.56 (m, 12H; hexyl), 1.73–1.95 (m, 4H; hexyl), 3.08 (t, $J = 7.5$ Hz, 4H; hexyl), 3.23 (s, 2H; ethynyl), 7.55 (d, $J = 8.1$ Hz, 4H; phenyl), 7.63 (d, $J = 8.1$ Hz, 4H; phenyl), 8.39 (s, 2H; phenanthroline), 9.06 ppm (s, 2H; phenanthroline); ^{13}C NMR (50 MHz): $\delta = 14.0$, 22.5, 29.1, 30.5, 31.6, 32.6, 79.5, 83.0, 85.7, 101.6, 123.0, 124.9, 125.0, 127.5, 131.6, 132.2, 132.5, 139.0, 144.3, 151.1 ppm; IR (KBr): = 3294, 3166, 2924, 2854, 2198, 2094, 1560, 1508, 1458, 1421, 1376, 1234, 1102, 893, 837, 754 cm^{-1}; elemental analysis calcd (%) for $C_{44}H_{40}N_2{\cdot}0.5\,H_2O$ (605.83): C 87.23, H 6.82, N 4.62; found: C 87.16, H 7.23, N 4.68.

4,7-Bis-[4-(5-*tert*-butyl-3-iodo-2-methoxyphenylethynyl)phenylethynyl]-3,8-dihexyl-1,10-phenanthroline (7): A mixture of **5b** (200 mg (330 μmol) and **6**[35] (1.56 g, 3.75 mmol), dry benzene (7 mL), dry triethylamine (2 mL), and $[Pd(PPh_3)_4]$ (200 mg, 170 μmol) was refluxed for 3 d. Then the solvent was removed under reduced pressure. After taking up the residue in dichloromethane (100 mL) it was washed with aqueous KCN

 © 2004 Wiley-VCH Verlag GmbH & Co. KGaA, Weinheim

(100 mL, 2%) and later with water. The organic layer was dried over $MgSO_4$ and the residual material subjected to column chromatography with first dichloromethane and later methyl-*tert*-butylether as eluents to give 340 mg of **7** (88%) as colourless powder. M.p. 208–210°C; ^{1}H NMR (200 MHz): δ=0.89 (t, J=6.9 Hz, 6H; hexyl), 1.24–1.57 (m, 12H; hexyl), 1.31 (s, 18H; *tert*-butyl), 1.72–1.97 (m, 4H; hexyl), 3.09 (t, J=8.3 Hz, 4H; hexyl), 4.02 (s, 6H; methoxy), 7.51 (d, J=2.3 Hz, 2H; phenyl), 7.62 (d, J=8.6 Hz, 4H; phenyl), 7.69 (d, J=8.6 Hz, 4H; phenyl), 7.77 (d, J=2.3 Hz, 2H; phenyl), 8.38 (s, 2H; phenanthroline), 9.05 ppm (s, 2H; phenanthroline); ^{13}C NMR (50 MHz): δ=14.0, 22.5, 29.1, 30.6, 31.2, 31.6, 32.6, 34.2, 61.0, 85.8, 88.1, 91.7, 93.2, 101.7, 116.2, 122.4, 124.0, 125.0, 127.5, 130.9, 131.6, 131.7, 131.9, 137.2, 138.9, 144.4, 148.6, 151.2, 158.1 ppm; IR (KBr):=3054, 2924, 2855, 2202, 1560, 1509, 1466, 1435, 1420, 1256, 1097, 1000, 835, 746, 693 cm^{-1}; elemental analysis calcd (%) for; $C_{66}H_{66}I_2N_2O_2$ (1173.07): C 67.58, H 5.67, N 2.39; found: C 67.68, H 5.86, N 2.41.

Synthesis of macrocycle 1: A solution of **7** (400 mg, 341 μmol) and **5b** (200 mg, 330 μmol) in dry benzene (20 mL) was added to a flask containing a mixture of $[Pd(PPh_3)_4]$ (350 mg, 300 μmol), dry benzene (60 mL) and dry triethylamine (20 mL) over a period of 32 h by means of an injection pump, while keeping at reflux. The resulting dark solution was refluxed for 8 h and the solvent was removed under reduced pressure. The obtained dark residue was suspended in trichloromethane and washed with aqueous KCN (100 mL, 2%). The aqueous phase was extracted several times with trichloromethane. The combined organic phases were evaporated to dryness under reduced pressure affording a residue which was then extracted twice with hot *n*-hexane (2×20 mL) and dried under reduced pressure. Subsequently, trichloromethane (5 mL) was added and after one night at room temperature colourless thin needles resulted, which were washed several times with trichloromethane to yield analytically pure **1** (80.0 mg, 16%). M.p. >300°C; ^{1}H NMR (200 MHz, $CDCl_3$/5% TFA): δ=0.93 (t, J=6.9 Hz, 12H; hexyl), 1.33–1.64 (m, 24H; hexyl), 1.40 (s, 18H; *tert*-butyl), 1.80–2.00 (m, 8H; hexyl), 3.25 (t, J=6.0 Hz, 8H; hexyl), 4.30 (s, 6H; methoxy), 7.61 (s, 4H; phenyl), 7.72 (d, J=8.6 Hz, 8H; phenyl), 7.80 (d, J=8.6 Hz, 8H; phenyl), 8.74 (s, 4H; phenanthroline), 9.10 ppm (s, 4H; phenanthroline); ^{13}C NMR ($CDCl_3$/5% TFA, 50 MHz): δ=13.9, 22.5, 29.2, 30.2, 31.2, 31.5, 32.8, 34.6, 62.1, 84.2, 88.6, 93.2, 109.8, 120.6, 126.0, 126.3, 126.4, 129.3, 131.3, 132.0, 132.5, 134.9, 135.0, 142.4, 146.8, 148.1, 160.1 ppm; IR (KBr):=3064, 3038, 2954, 2925, 2855, 2202, 1560, 1510, 1466, 1420, 1245, 1110, 1005, 880, 832, 752 cm^{-1}; ESI MS: m/z (%): 1515 (100) $[M+H]^+$; elemental analysis calcd (%) for $C_{110}H_{104}N_4O_2$ (1514.06): C 87.26, H 6.92, N 3.70; found: C 87.08, H 7.11, N 3.68.

2-(4-Methoxy-2,6-dimethylphenyl)-9-(2,4,6-trimethylphenyl)-1,10-phenanthroline (10): *n*-Butyllithium (2.5 M solution in hexane, 24.0 mL, 60.0 mmol) was added to a solution of 2-bromo-5-methoxy-1,3-dimethylbenzene (1.80 g, 8.37 mmol) in dry diethyl ether (20 mL) at 0°C. The yellow solution was stirred at room temperature for 1 h providing a colourless turbid mixture. Compound **9**[36] (1.00 g, 3.35 mmol) was then added slowly under nitrogen atmosphere over 15 min. The solution turned dark violet and was stirred for 18 h at room temperature. After quenching the reaction with H_2O (50 mL), the organic phase was separated. The aqueous phase layer was extracted with dichloromethane (50 mL), and the combined organic phases were dried over magnesium sulfate. The concentrated reaction mixture (volume: 50 mL) was subsequently oxidised with excess of activated MnO_2 (10 g) for 1 h and filtered through a pad of Celite with dichloromethane as eluent. After concentration of the filtrate the crude product was purified by column chromatography with first dichloromethane and then diethyl ether to give a 770 mg of a colourless solid (52%) M.p. 262°C; ^{1}H NMR (200 MHz): δ=2.17 (s, 6H; benzyl), 2.20 (s, 6H; benzyl), 2.33 (s, 3H; benzyl), 3.82 (s, 3H; methoxy), 6.68 (s, 2H; phenyl), 6.94 (s, 2H; phenyl), 7.57 (d, J=8.1 Hz, 1H; phenanthroline), 7.58 (d, J=8.3 Hz, 1H; phenanthroline), 7.84 (s, 2H; phenanthroline), 8.27 (d, J=8.1 Hz, 1H; phenanthroline), 8.28 ppm (d, J=8.3 Hz, 1H; phenanthroline); ^{13}C NMR (50 MHz): δ=20.5, 20.9, 21.0, 55.1, 113.1, 124.9, 125.2, 126.1, 127.0, 128.4, 133.9, 135.6, 136.2, 137.3, 137.9, 138.1, 146.2, 158.9, 159.8, 160.1 ppm; IR (KBr):=2953, 2915, 1606, 1583, 1541, 1479, 1375, 1356, 1319, 1194, 1156, 1100, 1074, 1039, 885, 858, 634 cm^{-1}; elemental analysis calcd (%) for $C_{30}H_{28}N_2O{\cdot}0.5\,H_2O$ (441.56): C 81.60, H 6.62, N 6.34; found: C 81.3, H 6.54, N 6.03.

3,5-Dimethyl-4-[9-(2,4,6-trimethylphenyl)-1,10-phenanthrolin-2-yl]phenol (12): Pyridine (9 mL) was added to conc. HCl (10.5 mL) and the resultant mixture was heated to reflux at 200°C (water was removed completely). After cooling the mixture to 140°C, **10** (400 mg, 906 μmol) was added. The mixture was heated to 215–220°C and kept there for 2.5 h. Subsequently, the mixture was cooled to 130°C and a solution of water (20 mL) and conc. HCl (5 mL) was added affording a yellow solution. After cooling to room temperature, the reaction mixture was extracted several times with dichloromethane. The organic phases were combined, washed with water and finally neutralised with conc. KOH. The organic layer was dried over $MgSO_4$ and the solvent was removed under reduced pressure. The residue was then purified by column chromatography with dichloromethane as eluent, furnishing 370 mg of **12** (96%) as a colourless powder. M.p. >280°C; ^{1}H NMR (200 MHz): δ=1.90 (s, 6H; benzyl), 2.12 (s, 6H; benzyl), 2.29 (s, 3H; benzyl), 6.30 (s, 2H; phenyl), 6.91 (s, 2H; phenyl), 7.51 (d, J=8.1 Hz, 1H; phenanthroline), 7.58 (d, J=8.3 Hz, 1H; phenanthroline), 7.86 (s, 2H; phenanthroline), 8.23 (d, J=8.3 Hz, 1H; phenanthroline), 8.34 ppm (d, J=8.1 Hz, 1H; phenanthroline); ^{13}C NMR (50 MHz): δ=20.3, 20.4, 21.1, 114.8, 123.8, 124.7, 125.5, 125.6, 126.4, 126.8, 127.1, 128.2, 131.2, 135.4, 135.8, 136.1, 136.4, 137.7, 145.6, 146.0, 156.9, 160.5, 161.1 ppm; IR (KBr):=3258,.3033, 2952, 2917, 2856, 1614, 1586, 1542, 1479, 1318, 1159, 1101, 1033, 887, 857, 756, 636 cm^{-1}; elemental analysis calcd (%) for $C_{29}H_{26}N_2O{\cdot}0.5\,H_2O$ (427.55): C 81.47, H 6.37, N 6.55; found: C 81.21, H 6.67, N 6.34.

Synthesis of 2: Anhydrous K_2CO_3 (300 mg, 2.17 mmol) was added at room temperature and in an inert atmosphere to a solution of **12** (600 mg, 1.43 mmol) and **13**[37] (410 mg, 610 μmol) in dry DMF (50 mL). The resulting dark brown solution was stirred for 1 h at room temperature and then for 3 d at 60–70°C. The solvent was evaporated under reduced pressure and taken up in a mixture of dichloromethane (100 mL) and water (100 mL). The organic layers were washed with water and dried over $MgSO_4$, then the solvent was evaporated to dryness. The residue was then subjected to column chromatography with first diethyl ether and later ethyl acetate as eluents to afford 520 mg (69%) of a beige powder. M.p. 87–89°C; ^{1}H NMR (200 MHz): δ=2.14 (s, 12H; benzyl), 2.15 (s, 12H; benzyl), 2.31 (s, 6H; benzyl), 3.65–3.78 (m, 8H; ethoxy), 3.80–3.94 (m, 8H; ethoxy), 4.02–4.19 (m, 8H; ethoxy), 6.66 (s, 4H; phenyl), 6.85 (s, 4H; phenyl), 6.93 (s, 4H; phenyl), 7.55 (d, J=8.1 Hz, 2H; phenanthroline), 7.57 (d, J=8.1 Hz, 2H; phenanthroline), 7.84 (s, 4H; phenanthroline), 8.26 (d, J=8.1 Hz, 2H; phenanthroline), 8.27 ppm (d, J=8.1 Hz, 2H; phenanthroline); ^{13}C NMR (50 MHz): δ=20.5, 20.9, 21.0, 67.3, 68.1, 69.7, 69.8, 70.7, 70.8, 113.9, 115.6, 124.9, 125.2, 126.1, 127.0, 128.4, 134.0, 135.6, 136.1, 137.3, 137.9, 138, 146, 153.1, 158.1, 159.7, 160.1 ppm; IR (KBr):=3036, 2917, 2856, 1604, 1585, 1508, 1476, 1317, 1231, 1164, 1125, 1069, 857, 634 cm^{-1}; elemental analysis calcd (%) for $C_{76}H_{78}N_4O_8{\cdot}3\,H_2O$ (1229.52): C 74.24, H 6.89, N 4.56; found: C 74.50, H 6.51, N 4.30.

Synthesis of complex C1: Tetrakis(acetonitrile)copper(I) hexafluorophosphate (25.0 mg, 67.0 μmol) in dichloromethane (10 mL) was added to a mixture of macrocycle **1** (50.7 mg, 33.5 μmol) and **11**[15b] (28.0 mg, 67.0 μmol). The resulting dark red solution was heated for several seconds, and the solvent was evaporated to give **C1**. After chromatography (silica gel; dichoromethane/methanol=10:1) 40.0 mg (43%) of a dark red powder were obtained. M.p. >300°C; ^{1}H NMR (600 MHz, CD_2Cl_2): δ=0.90 (t, J=7.1 Hz, 12H; hexyl), 1.32–1.44 (m, 16H; hexyl), 1.38 (s, 18H; *tert*-butyl), 1.45–1.52 (m, 8H; hexyl), 1.72 (s, 12H; benzyl), 1.74 (s, 24H; benzyl), 1.77–1.85 (m, 8H; hexyl), 3.08 (t, J=6.9 Hz, 8H; hexyl), 4.27 (s, 6H; methoxy), 6.05 (s, 8H; phenyl), 7.58 (s, 4H; phenyl), 7.73 (d, J=7.9 Hz, 8H; phenyl), 7.81 (d, J=7.9 Hz, 8H; phenyl), 7.82 (d, J=8.1 Hz, 4H; phenanthroline), 8.27 (s, 4H; phenanthroline), 8.37 (s, 4H; phenanthroline), 8.50 (s, 4H; phenanthroline), 8.74 ppm (d, J=8.1 Hz, 4H; phenanthroline); ^{13}C NMR (CD_2Cl_2, 151 MHz): δ=14.0, 20.0, 20.7, 22.5, 29.1, 30.7, 31.2, 31.6, 32.5, 34.4, 61.7, 84.7, 88.7, 92.9, 104.6, 116.5, 121.3, 125.1, 125.2, 126.4, 127.0, 127.9, 128.1, 131.0, 131.9, 132.1, 134.4, 137.0, 137.7, 137.8, 140.5, 141.4, 143.8, 146.7, 147.9, 158.7, 160.2 ppm; IR (KBr):=2965, 2922, 2854, 2194, 1582, 1509, 1458, 1420, 1244, 1105, 1008, 840, 557 cm^{-1}; ESI MS: m/z (%): 1236.4 (100) $[M-2\,PF_6]^+$; elemental analysis calcd (%) for $C_{170}H_{160}N_8O_2Cu_2P_2F_{12}$ (2764.21): C 73.87, H 5.83, N 4.05; found: C 73.41, H 6.22, N 4.07.

Synthesis of complex C2: Compound **10** (33.9 mg, 78.3 μmol), $[Cu(CH_3CN)_4]PF_6$ (29.2 mg, 78.3 μmol), and macrocycle **1** (59.3 mg,

© 2004 Wiley-VCH Verlag GmbH & Co. KGaA, Weinheim

39.1 μmol) were stirred for 1 h in dichloromethane (10 mL). The resulting dark red solution was evaporated to dryness to furnish **C2**. After chromatography (silica gel; dichoromethane/methanol = 10:1) 87.0 mg (80 %) of a dark red powder containing water were obtained. M.p. > 300 °C; ^{1}H NMR (600 MHz, CD_2Cl_2): δ = 0.91 (t, J = 7.2 Hz, 12 H; hexyl), 1.33–1.45 (m, 16 H; hexyl), 1.40 (s, 18 H; *tert*-butyl), 1.48–1.54 (m, 8 H; hexyl), 1.73 (s, 12 H; benzyl), 1.75 (s, 12 H; benzyl), 1.81 (s, 12 H; benzyl), 1.82–1.86 (m, 8 H; hexyl), 3.11 (t, J = 7.5 Hz, 8 H; hexyl), 3.34 (s, 6 H; methoxy), 4.27 (s, 6 H; methoxy), 5.83 (s, 4 H; phenyl), 6.07 (s, 4 H; phenyl), 7.63 (s, 4 H; phenyl), 7.77 (d, J = 8.1 Hz, 8 H; phenyl), 7.85 (d, J = 8.1 Hz, 8 H; phenyl), 7.86 (d, J = 8.0 Hz, 2 H; phenanthroline), 7.87 (d, J = 8.0 Hz, 2 H; phenanthroline), 8.25 (s, 4 H; phenanthroline), 8.40 (s, 4 H; phenanthroline), 8.53 (s, 4 H; phenanthroline), 8.72 (d, J = 8.0 Hz, 2 H; phenanthroline), 8.73 ppm (d, J = 8.0 Hz, 2 H; phenanthroline); ^{13}C NMR (CD_2Cl_2, 151 MHz): δ = 14.2, 20.2, 20.6, 20.8, 23.0, 29.6, 31.1, 31.3, 32.0, 33.0, 34.7, 55.0, 62.0, 85.3, 89.1, 93.1, 104.8, 112.0, 116.9, 122.0, 125.5, 125.6, 126.9, 127.1, 127.4, 128.4, 128.5, 128.6, 131.6, 132.3, 132.5, 133.1, 134.9, 136.7, 137.5, 137.9, 138.3, 141.2, 141.9, 144.4, 147.4, 148.5, 159.2, 159.3, 159.5, 160.6 ppm; IR (KBr): = 2954, 2923, 2855, 2195, 1654, 1570, 1508, 1475, 1458, 1420, 1320, 1245, 1156, 1104, 1011, 839, 558 cm^{-1}; ESI MS: m/z (%): 1253.2 (100) $[M-2PF_6]^+$; elemental analysis calcd (%) for $C_{170}H_{160}N_8O_4Cu_2P_2F_{12}\cdot 3H_2O$ (2796.21): C 71.64, H 5.87, N 3.93; found: C 71.75, H 5.93, N 4.29.

Synthesis of complex C3: Compound **2** (49.0 mg, 40.9 μmol), **5a** (74.4 mg, 81.8 μmol) and $[Cu(CH_3CN)_4]PF_6$ (30.5 mg (81.8 μmol) were stirred in dry dichloromethane (10 mL) for 2 h. The resulting dark red solution was evaporated to afford crude **C3**. After chromatography (silica gel; dichoromethane/methanol = 10:1) 130 mg (85 %) of a dark red powder containing dichloromethane were obtained. M.p. > 122–124 °C; ^{1}H NMR (600 MHz, CD_2Cl_2): δ = 0.86–0.90 (m, 12 H; hexyl), 1.15–1.20 (m, 84 H; triisopropyl), 1.31–1.40 (m, 16 H; hexyl), 1.43–1.49 (m, 8 H; hexyl), 1.70–1.72 (m, 6 H; benzyl), 1.72–1.74 (m, 12 H; benzyl), 1.77–1.82 (m, 8 H; hexyl), 1.79 (s, 12 H; benzyl), 3.07 (t, J = 7.6 Hz, 8 H; hexyl), 3.55–3.56 (m, 4 H; ethoxy), 3.57 (s, 4 H; ethoxy), 3.58 (s, 4 H; ethoxy), 3.60–3.68 (m, 4 H; ethoxy), 3.69–3.81 (m, 4 H; ethoxy), 3.95–4.05 (m, 4 H; ethoxy), 5.84 (s, 4 H; phenyl), 6.02–6.06 (m, 4 H; phenyl), 6.75–6.80 (m, 4 H; phenyl), 7.59–7.63 (m, 8 H; phenyl), 7.71–7.74 (m, 8 H; phenyl), 7.85–7.94 (m, 4 H; phenanthroline), 8.24 (s, 4 H; phenanthroline), 8.38–8.40 (m, 4 H; phenanthroline), 8.47–8.52 (m, 4 H; phenanthroline), 8.70–8.74 ppm (m, 4 H; phenanthroline); ^{13}C NMR (151 MHz): δ = 11.7, 14.2, 18.8, 20.3, 20.6, 20.8, 23.0, 29.6, 31.1, 32.0, 33.0, 67.2, 68.3, 69.8, 70.1, 71.0, 71.1, 85.2, 94.9, 104.7, 106.6, 112.6, 115.7, 122.0, 125.6, 127.0, 127.2, 127.4, 128.3, 128.4, 128.6, 129.1, 132.2, 132.7, 133.3, 134.8, 136.7, 137.4, 137.9, 138.2, 141.4, 141.9, 144.4, 148.4, 153.4, 158.3, 159.2, 159.4 ppm; IR (KBr): = 2924, 2862, 2198, 2152, 1618, 1578, 1542, 1508, 1458, 1376, 1232, 1164, 1124, 1071, 839, 747, 557 cm^{-1}; ESI MS: m/z (%): 1560.3 (100) $[M-2PF_6]^+$; elemental analysis calcd (%) for $C_{200}H_{238}N_8O_8Si_4Cu_2P_2F_{12}\cdot 4CH_2Cl_2$ (3751.23): C 65.40, H 6.62, N 2.99; found: C 65.11, H 6.44, N 2.90.

Preparation of heteroleptic basket assembly C4: Tetrakis(acetonitrile)-copper(I) hexafluorophosphate (12.0 mg, 32.2 μmol) in dichloromethane (10 mL) was added to a mixture of **1** (24.2 mg, 16.1 μmol) and **2** (18.7 mg, 16.1 μmol). The resulting dark red solution was heated (~35 °C) for several seconds and then the solvent was evaporated to afford the basket assembly (**C4$_{xyz}$**) quantitatively as dark red powder (containing water). M.p. 225 °C; IR (KBr): = 2924, 2855, 2195, 1605, 1509, 1462, 1260, 1101, 1026, 839, 555 cm^{-1}; ESI MS (**C4$_{xyz}$**): m/z (%): 1408.4 (100) $[M-2PF_6]^+$; elemental analysis calcd (%) for $C_{186}H_{182}N_8O_{10}Cu_2P_2F_{12}\cdot 2H_2O$ (3142.59): C 71.09, H 5.97, N 3.57; found: C 71.02, H 5.89, N 3.46. **C4x**:**C4y**:**C4z** were formed in a 59:24:17 ratio. **C4x**,**y** could be separated from **C4z** by chromatography (silica gel, dichloromethane/methanol = 100:1). Initial fractions contained **C4x**,**y** as the sole products while later fractions furnished enriched **C4z** (80 %).

Isomer C4x: ^{1}H NMR (600 MHz, CD_2Cl_2): δ = 0.88–0.93 (m, 12 H; hexyl), 1.32–1.45 (m, 16 H; hexyl), 1.39 (s, 18 H; *tert*-butyl), 1.47–1.56 (m, 8 H; hexyl), 1.58 (s, 6 H; benzyl), 1.68 (s, 12 H; benzyl), 1.80–1.86 (m, 8 H; hexyl), 1.87 (s, 12 H; benzyl), 3.02–3.20 (m, 8 H; hexyl), 3.50–3.52 (m, 4 H; ethoxy), 3.53–3.56 (m, 4 H; ethoxy), 3.57–3.59 (m, 4 H; ethoxy), 3.69–3.70 (m, 4 H; ethoxy), 4.01–4.02 (m, 4 H; ethoxy), 4.16–4.20 (m, 4 H; ethoxy), 4.21 (s, 6 H; methoxy; H_{Xd}), 5.64 (s, 4 H; phenyl; H_{Xb}), 6.19 (s, 4 H; phenyl; H_{Xa}), 6.87 (s, 4 H; phenyl; H_{Xc}), 7.63 (s, 4 H; phenyl), 7.76–7.77 (m, 8 H; phenyl), 7.83 (d, J = 8.0 Hz, 2 H; phenanthroline), 7.84–7.86 (m, 8 H; phenyl), 7.93 (d, J = 8.2 Hz, 2 H; phenanthroline), 8.21 (d, J = 9.3 Hz, 2 H; phenanthroline; $H_{X6'}$), 8.24 (d, J = 9.3 Hz, 2 H; phenanthroline; $H_{X6'}$), 8.40 (s, 4 H; phenanthroline), 8.52 (s, 4 H; phenanthroline), 8.70 (d, J = 8.0 Hz, 2 H; phenanthroline), 8.74 ppm (d, J = 8.2 Hz, 2 H; phenanthroline); ^{13}C NMR (CD_2Cl_2, 151 MHz): δ = 14.0, 20.0, 20.3, 20.4, 23.0, 29.1, 29.3, 30.9, 31.7, 32.7, 34.5, 61.7, 66.7, 68.0, 68.1, 69.3, 70.5, 70.9, 85.0, 88.9, 92.8, 104.6, 111.8, 115.5, 116.6, 121.7, 125.2, 125.4, 126.8, 126.9, 127.3, 128.0, 128.1, 128.3, 131.4, 132.0, 132.2, 132.6, 132.9, 134.7, 136.2, 136.4, 137.5, 137.6, 138.1, 140.9, 141.6, 144.1, 147.2, 148.2, 153.2, 153.3, 157.8, 158.7, 160.3 ppm.

Isomer C4y: ^{1}H NMR (600 MHz, CD_2Cl_2): δ = 0.88–0.93 (m, 12 H; hexyl), 1.32–1.45 (m, 16 H; hexyl), 1.38 (s, 18 H; *tert*-butyl), 1.47–1.56 (m, 8 H; hexyl), 1.70 (s, 12 H; benzyl), 1.74 (s, 6 H; benzyl), 1.80–1.86 (m, 8 H; hexyl), 1.99 (s, 12 H; benzyl), 3.02–3.20 (m, 8 H; hexyl), 3.61–3.62 (m, 4 H; ethoxy), 3.63–3.65 (m, 4 H; ethoxy), 3.70–3.72 (m, 4 H; ethoxy), 3.78–3.80 (m, 4 H; ethoxy), 3.89–3.90 (m, 4 H; ethoxy), 3.96–3.98 (m, 4 H; ethoxy), 4.14 (s, 6 H; methoxy; H_{Yc}), 5.49 (s, 4 H; phenyl; H_{Yb}), 6.33 (s, 4 H; phenyl; H_{Ya}), 7.07 (s, 4 H; phenyl; H_{Yc}), 7.62 (s, 4 H; phenyl), 7.74–7.76 (m, 8 H; phenyl), 7.77 (d, J = 8.1 Hz, 2 H; phenanthroline), 7.87–7.88 (m, 8 H; phenyl), 7.97 (d, J = 8.2 Hz, 2 H; phenanthroline), 8.21 (d, J = 9.3 Hz, 2 H; phenanthroline; $H_{Y6'}$), 8.24 (d, J = 9.3 Hz, 2 H; phenanthroline; $H_{Y5'}$), 8.40 (s, 4 H; phenanthroline), 8.55 (s, 4 H; phenanthroline), 8.67 (d, J = 8.1 Hz, 2 H; phenanthroline), 8.76 ppm (d, J = 8.2 Hz, 2 H; phenanthroline); ^{13}C NMR (CD_2Cl_2, 151 MHz): δ = 13.9, 20.1, 20.3, 20.4, 23.0, 29.1, 29.3, 30.9, 31.7, 32.7, 34.5, 61.6, 66.6, 69.8, 70.5, 70.8, 71.2, 71.3, 85.0, 88.9, 92.8, 104.6, 111.5, 115.7, 116.6, 121.8, 125.3, 125.4, 126.8, 127.6, 128.0, 128.1, 128.3, 131.3, 132.0, 132.2, 132.6, 132.9, 134.7, 136.2, 136.4, 137.5, 137.8, 138.1, 140.9, 141.6, 144.1, 147.2, 148.2, 153.2, 153.3, 157.8, 159.3, 160.4 ppm.

Isomer C4z: ^{1}H NMR (400 MHz, CD_2Cl_2): δ = 0.79–0.83 (m, 12 H; hexyl), 1.32–1.45 (m, 16 H; hexyl), 1.38 (s, 18 H; *tert*-butyl), 1.47–1.56 (m, 8 H; hexyl), 1.70 (s, 12 H; benzyl), 1.74 (s, 6 H; benzyl), 1.80–1.86 (m, 8 H; hexyl), 1.99 (s, 12 H; benzyl), 2.91–3.01 (m, 8 H; hexyl), 3.61–3.62 (m, 4 H; ethoxy), 3.63–3.65 (m, 4 H; ethoxy), 3.70–3.72 (m, 4 H; ethoxy), 3.78–3.80 (m, 4 H; ethoxy), 3.89–3.90 (m, 4 H; ethoxy), 3.96–3.98 (m, 4 H; ethoxy), 4.24 (s, 6 H; methoxy; H_{za}), 5.85 (s, 4 H; phenyl; H_{Zb}), 6.06 (s, 4 H; phenyl), 6.75 (s, 4 H; phenyl; H_{Zc}), 7.61 (s, 4 H; phenyl), 7.75–7.77 (m, 8 H; phenyl), 7.77 (d, J = 8.1 Hz, 2 H; phenanthroline), 7.87–7.88 (m, 8 H; phenyl), 7.97 (d, J = 8.2 Hz, 2 H; phenanthroline), 8.21 (d, J = 9.3 Hz, 2 H; phenanthroline; $H_{Z5'}$), 8.23 (s, 2 H; phenanthroline; $H_{Z6'}$), 8.38 (s, 4 H; phenanthroline), 8.53 (s, 4 H; phenanthroline), 8.67 (d, J = 8.1 Hz, 2 H; phenanthroline), 8.76 ppm (d, J = 8.2 Hz, 2 H; phenanthroline).

Acknowledgement

We are indebted to the financial support from the DFG, the Fonds der Deutschen Chemie and the European Union (MAC-MES).

[1] a) B. Dietrich, P. Viout, J.-M. Lehn, *Macrocyclic Chemistry*, VCH, Weinheim **1993**; b) *Macrocycle Synthesis*, (Ed.: D. Parker), Oxford University Press, Oxford **1996**.

[2] S. Höger, K. Bonrad, A. Mourran, U. Beginn, M. Möller, *J. Am. Chem. Soc.* **2001**, *123*, 5651 – 5659.

[3] E. Mena-Osteritz, P. Bäuerle, *Adv. Mater.* **2001**, *13*, 243 – 246.

[4] P. Samori, F. Jäckel, O. Unsal, A. Godt, J. P. Rabe, *ChemPhysChem* **2001**, *2*, 461 – 464.

[5] a) A. S. Shetty, P. R. Fischer, K. F. Stork, P. W. Bohn, J. S. Moore, *J. Am. Chem. Soc.* **1996**, *118*, 9409 – 9414; b) O. Y. Mindyuk, M. R. Stetzer, D. Gidalevitz, P. A. Heiney, *Langmuir* **1999**, *15*, 6897 – 6900; c) Krömer, I. Rios-Carreras, G. Fuhrmann, C. Musch, M. Wunderlin, T. Debaerdemaeker, E. Mena-Osteritz, P. Bäuerle, *Angew. Chem.* **2000**, *112*, 3623 – 3628; *Angew. Chem. Int. Ed.* **2000**, *39*, 3481 – 3486.

[6] a) S. Höger, *J. Polym. Sci. Part A: Polym. Chem.* **1999**, *37*, 2685 – 2698; b) F. Diederich, *Nature* **1994**, *369*, 199 – 207; c) J. M. Tour, *Chem. Rev.* **1996**, *96*, 537 – 553. d) J. S. Moore, *Acc. Chem. Res.* **1997**, *30*, 402 – 413; e) M. M. Haley, *Synlett* **1998**, 557 – 565; f) M. M. Haley, J. J. Pak, S. C. Brand, *Top. Curr. Chem.* **1999**, *201*, 81 – 130; g) F. Die-

 © 2004 Wiley-VCH Verlag GmbH & Co. KGaA, Weinheim

derich, *Chem. Commun.* **2001**, 219–227; h) C. Grave, A. D. Schlüter, *Eur. J. Org. Chem.* **2002**, 3075–3098; P. N. W. Baxter, *Chem. Eur. J.* **2003**, *9*, 5011–5022; i) Y. Yamaguchi, Z. Yoshida, *Chem. Eur. J.* **2003**, *9*, 5430–5440; j) S. Höger, *Chem. Eur. J.* **2004**, *10*, 1320–1329.

[7] a) M. Schmittel, H. Ammon, V. Kalsani, A. Wiegrefe, C. Michel, *Chem. Commun.* **2002**, 2566–2567; b) O. Henze, D. Lentz, A. Schäfer, P. Franke, A. D. Schlüter, *Chem. Eur. J.* **2002**, *8*, 357–365; c) K. Campbell, R. McDonald, N. R. Branda, R. R. Tykwinski, *Org. Lett.* **2001**, *3*, 1045–1048; d) K. Campbell, C. J. Kuehl, M. J. Ferguson, P. J. Stang, R. R. Tykwinski, *J. Am. Chem. Soc.* **2002**, *124*, 7266–7267; e) P. H. Ge, W. Fu, W. A. Herrmann, E. Herdtweck, C. Campana, R. D. Adams, U. H. F. Bunz, *Angew. Chem.* **2000**, *112*, 3753–3756; *Angew. Chem. Int. Ed.* **2000**, *39*, 3607–3610; f) S. Höger, V. Enkelmann, K. Bonrad, C. Tschierske, *Angew. Chem.* **2000**, *112*, 2355–2358; *Angew. Chem. Int. Ed.* **2000**, *39*, 2267–2270; g) O. Henze, D. Lentz, A. D. Schlüter, *Chem. Eur. J.* **2000**, *6*, 2362–2367; h) M. Ohkita, K. Ando, T. Suzuki, T. Tsuji, *J. Org. Chem.* **2000**, *65*, 4385–4390; i) M. J. Marsella, I. T. Kim, F. Tham, *J. Am. Chem. Soc.* **2000**, *122*, 974–975; j) Y. Tobe, T. Fujii, H. Matsumoto, K. Tsumuraya, D. Noguchi, N. Nakagawa, M. Sonoda, K. Naemura, Y. Achiba, T. Wakabayashi, *J. Am. Chem. Soc.* **2000**, *122*, 1762–1775; k) S. Eisler, R. R. Tykwinski, *Angew. Chem.* **1999**, *111*, 2138–2141; *Angew. Chem. Int. Ed.* **1999**, *38*, 1940–1943; l) T. Kawase, Y. Hosokawa, H. Kurata, M. Oda, *Chem. Lett.* **1999**, 745–746; m) M. Haley, S. C. Brand, J. J. Pak, *Angew. Chem.* **1997**, *109*, 863–866; *Angew. Chem. Int. Ed. Engl.* **1997**, *36*, 835–838; n) J. Anthony, A. M. Boldi, C. Boudon, J.-P. Gisselbrecht, M. Gross, P. Seiler, C. B. Knobler, F. Diederich, *Helv. Chim. Acta* **1995**, *78*, 797–817.

[8] a) C. Dietrich-Buchecker, J.-P. Sauvage, *Chem. Rev.* **1987**, *87*, 795–810; b) B. X. Colasson, C. Dietrich-Buchecker, M. C. Jimenez-Molero, J.-P. Sauvage, *J. Phys. Org. Chem.* **2002**, *15*, 476–483; c) V. Balzani, A. Credi, F. M. Raymo, J. F. Stoddart, *Angew. Chem.* **2000**, *112*, 3486–3531; *Angew. Chem. Int. Ed.* **2000**, *39*, 3348–3391.

[9] B. Meynhardt, U. Lüning, C. Wolff, C. Näther, *Eur. J. Org. Chem.* **1999**, *9*, 2327–2335.

[10] a) C. Dietrich-Buchecker, G. Rapenne, J.-P. Sauvage, *Coord. Chem. Rev.* **1999**, *185–186*, 167–176; b) H. J. Claude, C. Dietrich-Buchecker, J.-P. Sauvage, *Compr. Supramol. Chem.* **1996**, *9*, 43–83.

[11] U. Velten, M. Rehahn, *Macromol. Chem. Phys.* **1998**, *199*, 127–140.

[12] M. Schmittel, H. Ammon, *Synlett* **1999**, 750–752.

[13] M. Schmittel, H. Ammon, *Synlett* **1997**, 1096–1098.

[14] a) E. Leize, D. R. Dorsselaer, R. Krämer, J.-M. Lehn, *J. Chem. Soc. Chem. Commun.* **1993**, 990–993; b) T. Bark, T. Weyhermüller, F. Heirtzler, *Chem. Commun.* **1998**, 1475–1476.

[15] a) M. Schmittel, A. Ganz, *Chem. Commun.* **1997**, 99–100; b) M. Schmittel, U. Lüning, M. Meder, A. Ganz, C. Michel, M. Herderich, *Heterocycl. Commun.* **1997**, *3*, 493–498.

[16] C. Dietrich-Buchecker, P. A. Marnot, J.-P. Sauvage, *Tetrahedron Lett.* **1982**, *23*, 5291–5294.

[17] R. Lazzaroni, A. Calderone, J. L. Bredas, J. P. Rabe, *J. Chem. Phys.* **1997**, *107*, 99–105.

[18] a) R. J. P. Williams, *J. Chem. Soc.* **1955**, 137–145; b) R. A. Palmer, T. S. Piper, *Inorg. Chem.* **1966**, *5*, 864–878; c) W. R. McWinnie, J. D. Miller, *Adv. Inorg. Chem. Radiochem.* **1969**, *12*, 135.

[19] a) V. Goulle, R. P. Thummel, *Inorg. Chem.* **1990**, *29*, 1767–1772; b) M. Schmittel, C. Michel, S. X. Liu, D. Schildbach, D. Fenske, *Eur. J. Inorg. Chem.* **2001**, 1155–1166; c) X. Y. Li, J. Illigen, M. Nieger, S. Michel, C. A. Schalley, *Chem. Eur. J.* **2003**, *9*, 1332–1347.

[20] P. N. W. Baxter, J.-M. Lehn, G. Baum, D. Fenske, *Chem. Eur. J.* **1999**, *5*, 102–112 and references therein.

[21] N. Fatin Rouge, S. Blanc, A. Pfeil, A. Rigault, A. M. Albrecht-Gary, J.-M. Lehn, *Helv. Chim. Acta* **2001**, *84*, 1694–1711.

[22] Combining **1**, **2** and copper(I) salt at −60 °C leads to a ratio of **C4x**:**C4y**:**C4z** = 45:20:35 (determined at room temperature).

[23] Hyperchem® 6.02 Release for Windows by Hypercube, Inc. 2000. MM+ force field.

[24] The ^{1}H NMR data of **C4xy** for proton H_a, H_b and H_d suggest that in **C4y** the distortion at the Cu^+ centre is even more pronounced than in **C4x**. This could be explained by assuming a planar macrocycle in **C4x** and a slightly folded one in **C4y**.

[25] This limitation is due to the fact that 3,8-dihexyl groups at the phenanthroline of **1** are prohibiting a sideward slide-on motion.

[26] Most likely, π–π and other attractive interactions as well as desolvation effects stabilize **model II** and its precursor complexes.

[27] M. Schmittel, A. Ganz, *Org. Lett.* **2002**, *4*, 2289–2292.

[28] A. Marquis-Rigault, A. Dupont-Gervais, P. N. W. Baxter, A. Van-Dorsselaer, J.-M. Lehn, *Inorg. Chem.* **1996**, *35*, 2307–2310.

[29] M. Schmittel, A. Ganz, V. Kalsani, *unpublished results.*

[30] a) H. Gampp, M. Maeder, C. J. Meyer, A. D. Zuberbühler, *Talanta* **1985**, *32*, 95–101; b) F. J. C. Rossoti, H. S. Rossoti, R. J. Whewell, *J. Inorg. Nucl. Chem.* **1971**, *33*, 2051–2065; c) H. Gampp, M. Maeder, C. J. Meyer, A. D. Zuberbühler, *Talanta* **1985**, *32*, 257–264d) H. Gampp, M. Maeder, C. J. Meyer, A. D. Zuberbühler, *Talanta* **1986**, *33*, 943–951.

[31] J. L. Burmeister, F. Basolo, *Inorg. Chem.* **1964**, *3*, 1587–1593.

[32] D. R. Coulson, *Inorg. Synth.* **1972**, *13*, 121–124.

[33] A. Godt, *J. Org. Chem.* **1997**, *62*, 7471–7474.

[34] J. P. Rabe, S. Buchholz, *Science* **1991**, *253*, 424–427.

[35] R. C. Helgeson, B. J. Selle, I. Goldberg, C. B. Knobler, D. J. Cram, *J. Am. Chem. Soc.* **1993**, *115*, 11506–11511.

[36] M. Schmittel, A. Ganz, D. Fenske, M. Herderich, *J. Chem. Soc. Dalton Trans.* **2000**, 353–359.

[37] P. L. Anelli, P. R. Ashton, N. Spencer, A. M. Z. Slawin, J. F. Stoddart, D. J. Williams, *Angew. Chem.* **1991**, *103*, 1052–1054; *Angew. Chem. Int. Ed. Engl.* **1991**, *30*, 1036–1039.

Received: December 2, 2003
Revised: June 23, 2004
Published online: September 20, 2004

 © 2004 Wiley-VCH Verlag GmbH & Co. KGaA, Weinheim